nature immunology

SUPPLEMENTARY INFORMATION

https://doi.org/10.1038/s41590-018-0259-z

In the format provided by the authors and unedited.

A TCR mechanotransduction signaling loop induces negative selection in the thymus

Jinsung Hong[1,2,9,13], Chenghao Ge[2,3,13], Prithiviraj Jothikumar[2,3], Zhou Yuan[2,3], Baoyu Liu[2,3,10], Ke Bai[2,3,11], Kaitao Li[2,3], William Rittase[1,2], Miho Shinzawa[4], Yun Zhang[5], Amy Palin[6,12], Paul Love[6], Xinhua Yu[7], Khalid Salaita[5], Brian D. Evavold[8,10], Alfred Singer[4] and Cheng Zhu[1,2,3]*

[1]Woodruff School of Mechanical Engineering, Georgia Institute of Technology, Atlanta, GA, USA. [2]Petit Institute of Bioengineering and Bioscience, Georgia Institute of Technology, Atlanta, GA, USA. [3]Coulter Department of Biomedical Engineering, Georgia Institute of Technology, Atlanta, GA, USA. [4]Experimental Immunology Branch, National Cancer Institute, National Institutes of Health, Bethesda, MD, USA. [5]Department of Chemistry, Emory University, Atlanta, GA, USA. [6]Section on Hematopoiesis and Lymphocyte Biology, Eunice Kennedy Shriver National Institute of Child Health and Development, National Institutes of Health, Bethesda, MD, USA. [7]Division of Epidemiology, Biostatistics and Environment Health, University of Memphis, Memphis, TN, USA. [8]Department of Immunology and Microbiology, Emory University School of Medicine, Atlanta, GA, USA. [9]Present address: Vaccine Production Program Laboratory, Vaccine Research Center, National Institute of Allergy and Infectious Diseases, National Institute of Health, Gaithersburg, MD, USA. [10]Present address: Department of Pathology, University of Utah School of Medicine, Salt Lake City, UT, USA. [11]Present address: Vaccine Research Center, National Institute of Allergy and Infectious Diseases, National Institute of Health, Bethesda, MD, USA. [12]Present address: Experimental Immunology Branch, National Cancer Institute National Institutes of Health, Bethesda, MD, USA. [13]These authors contributed equally: Jinsung Hong, Chenghao Ge. *e-mail: cheng.zhu@bme.gatech.edu

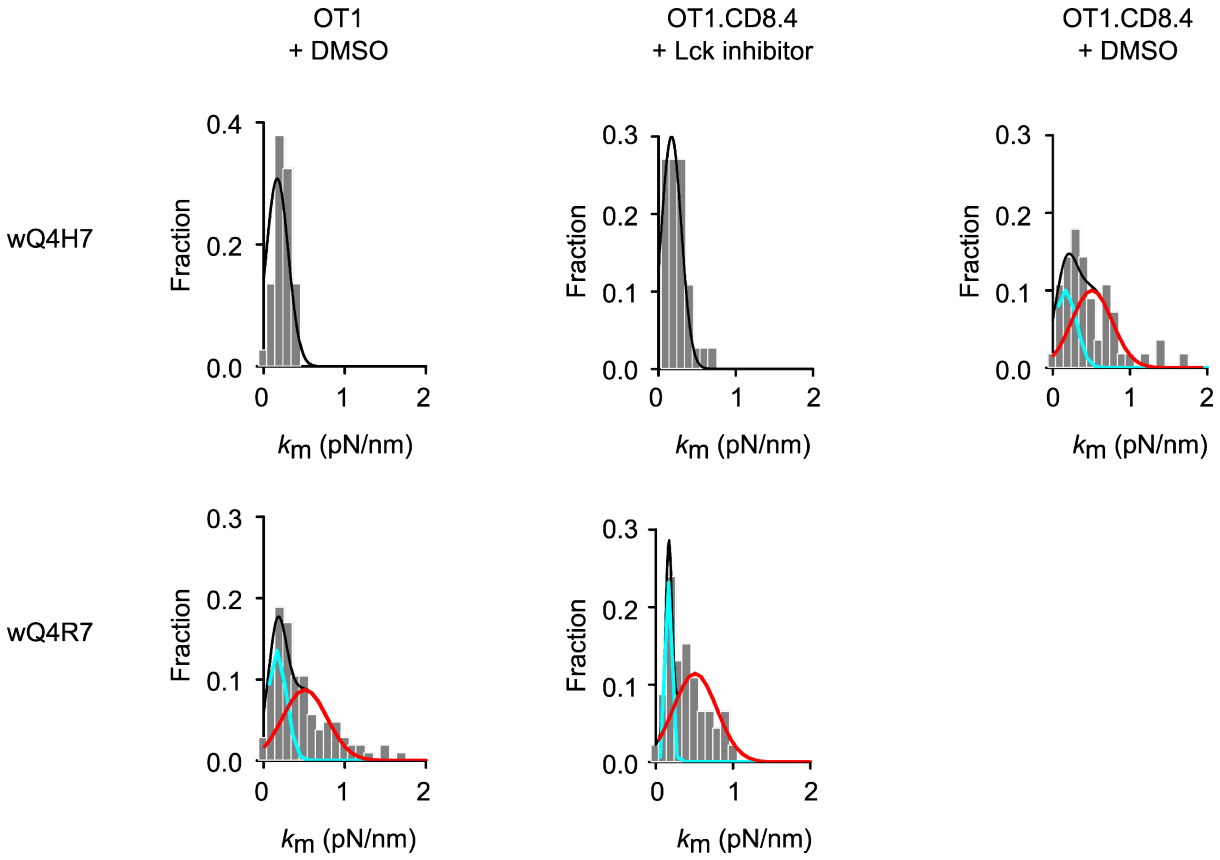

Supplementary Figure 1

Lck inhibition eliminated trimolecular bonds of CD8.4 thymocytes with wQ4H7 but not with wQ4R7, Related to Fig. 2.

Molecular stiffness histograms of complexes of DMSO-treated OT1 (first column), Lck inhibitor-treated OT1.CD8.4 (second column) and DMSO-treated OT1.CD8.4 (third column) thymocytes with wQ4H7 (upper row) or wQ4R7 (bottom row). Data (bar) were fitted by a single or double Gaussian per panel. The fitting parameters and statistics for their comparisons are summarized in Supplementary Tables 4a, 4b and 5a, respectively.

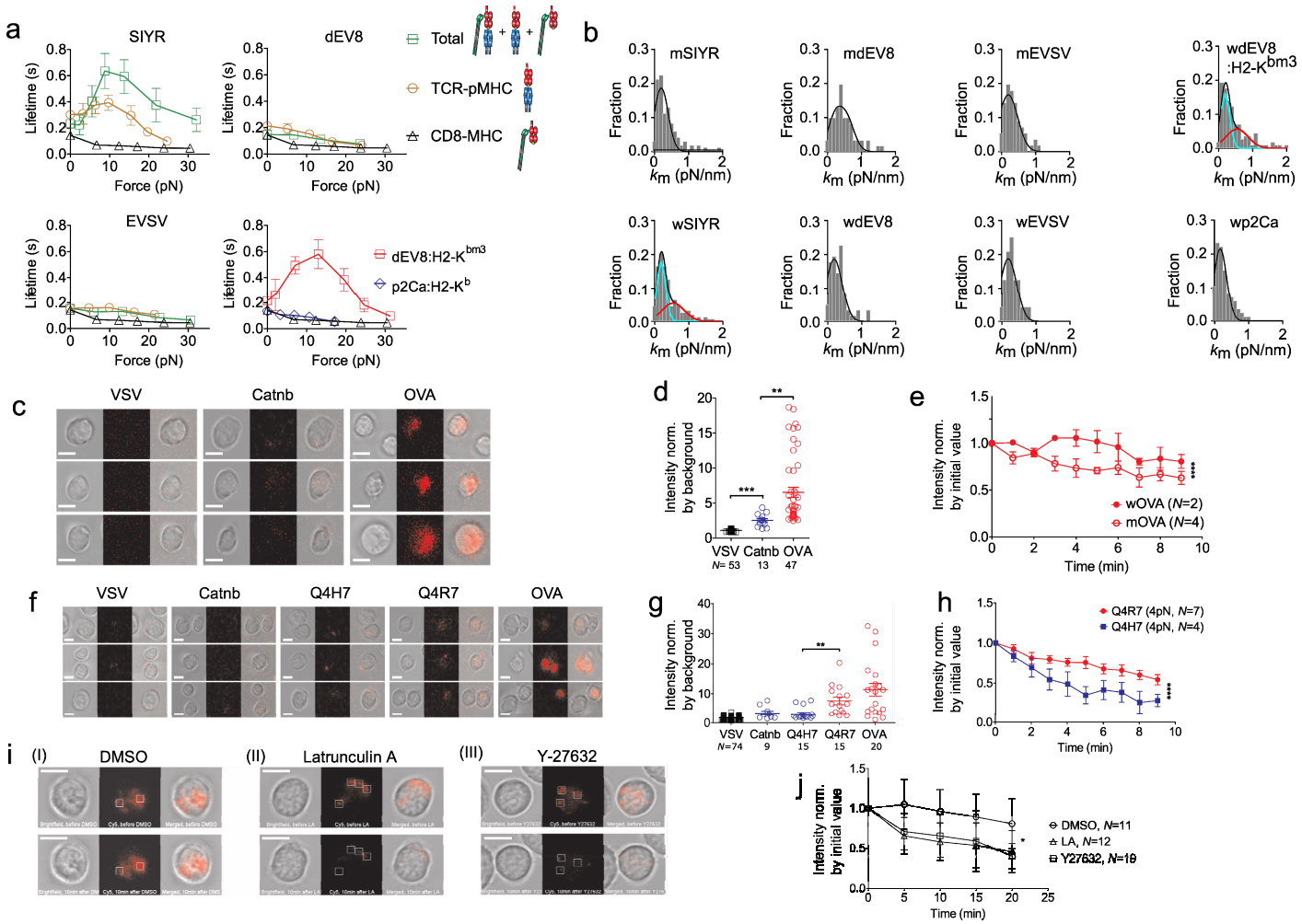

Supplementary Figure 2

Further confirmation of the thymocyte negative selection criteria by force-dependent bond lifetimes, molecular stiffness and cell pulling, Related Fig. 4.

a, Mean ± s.e.m. of lifetime versus force plots of total bonds with indicated peptides presented by H2-K^b (green square and blue diamond) or H2-K^{bm3} (red square), TCR bonds with three peptides presented by H2-K^{b}α3A2 (brown circle), and CD8 bond with VSV:H-2K^b (black triangle) measured using 2C TCR transgenic mice. The total bonds with the negative selecting ligands, SIYR:H-2K^b and dEV8:H-2K^{bm3}, exhibited catch bond behavior at low forces whereas those with the positive selecting ligands, dEV8, EVSV and p2Ca bound to H-2K^b, showed slip bond behavior[9, 10, 11, 52]. Like mOVA, the super agonist SIYR also formed catch bond at low forces with the 2C TCR in the absence of CD8, but the other two pMHC bimolecular interactions and the MHC–CD8 interaction form slip bonds. The numbers of bond lifetime measurements per curve for different ligands, the results of statistical tests examining the trends of the curves and their differences are summarized in Supplementary Tables 1d, 2c and 3a, b, respectively. **b**, Molecular stiffness histograms of 2C TCR bimolecular complexes with the indicated peptides bound to H-2K^{b}α3A2, total complexes with these peptides bound to H-2K^b, and total complexes with dEV8:H-2K^{bm3} and p2Ca:H-2K^b. Data (bar) were fitted by a single (black curve) or double (black curve = cyan curve + red curve) Gaussian. The fitting parameters and statistics for their comparisons are summarized in Supplementary Tables 4c and 5c, respectively. **c**, Representative images of thymocytes placed on wVSV, wCatnb, and wOVA tagged with a 13.1 pN MTP viewed in the bright-field (left column), fluorescence (middle column), and merged (right column) channels. Scale bar = 5 μm. **d**, Comparison of initial force signals from wVSV, wCatnb, and wOVA tagged with a 13.1 pN MTP. **e**, Comparison of force signal decays of OT1 thymocytes pulled on mOVA and wOVA tagged with a 13.1 pN MTP. **f**, Representative images of thymocytes pulled on indicated peptides presented by H-2K^b tagged with a 4.7 pN MTP viewed in the bright-field (left column), fluorescence (middle column), and merged (right column) channels. Scale bar = 5 μm. **g**, Comparison of normalized fluorescence intensity (points, left ordinate) and fraction of positive cells (bars, right ordinate) for indicated peptides bound to H2-K^b. Normalized fluorescence intensity was calculated by dividing the mean fluorescence intensity from a Cy5 positive cell by the background. Data are presented as mean ± s.e.m of all

positive cells (each cell is represented by a point with *N* indicating the number of positive cells). **h**, Comparison of force signal decays of OT1 thymocytes pulled on wQ4H7 and wQ4R7 tagged by a 4.7 pN MTP. **i**, Representative images of OT1 thymocytes pulled on wOVA tagged with a 13.1 pN MTP treated with the indicated agents: DMSO control, actin polymerization inhibitor latruculin A, and ROCK inhibitor Y-27632. OT1 thymocytes before (top row) and 10 min after (bottom row) the drug treatment were viewed in the bright-field (left column), fluorescence (middle column), and merged (right column) channels. Scale bar = 5 μm. **j**, Comparison of force signal decays of OT1 thymocytes pulled on wOVA over 20 min for the same treatments as in (**i**). Data in (**e**, **h**, **j**) are presented as mean ± s.e.m. of fluorescence intensity normalized by the initial value at 0 min (*N* = number of cell pooled from at least two independent experiments). *and **** denote $p < 0.05$ and 0.0001, respectively, by two-way ANOVA.

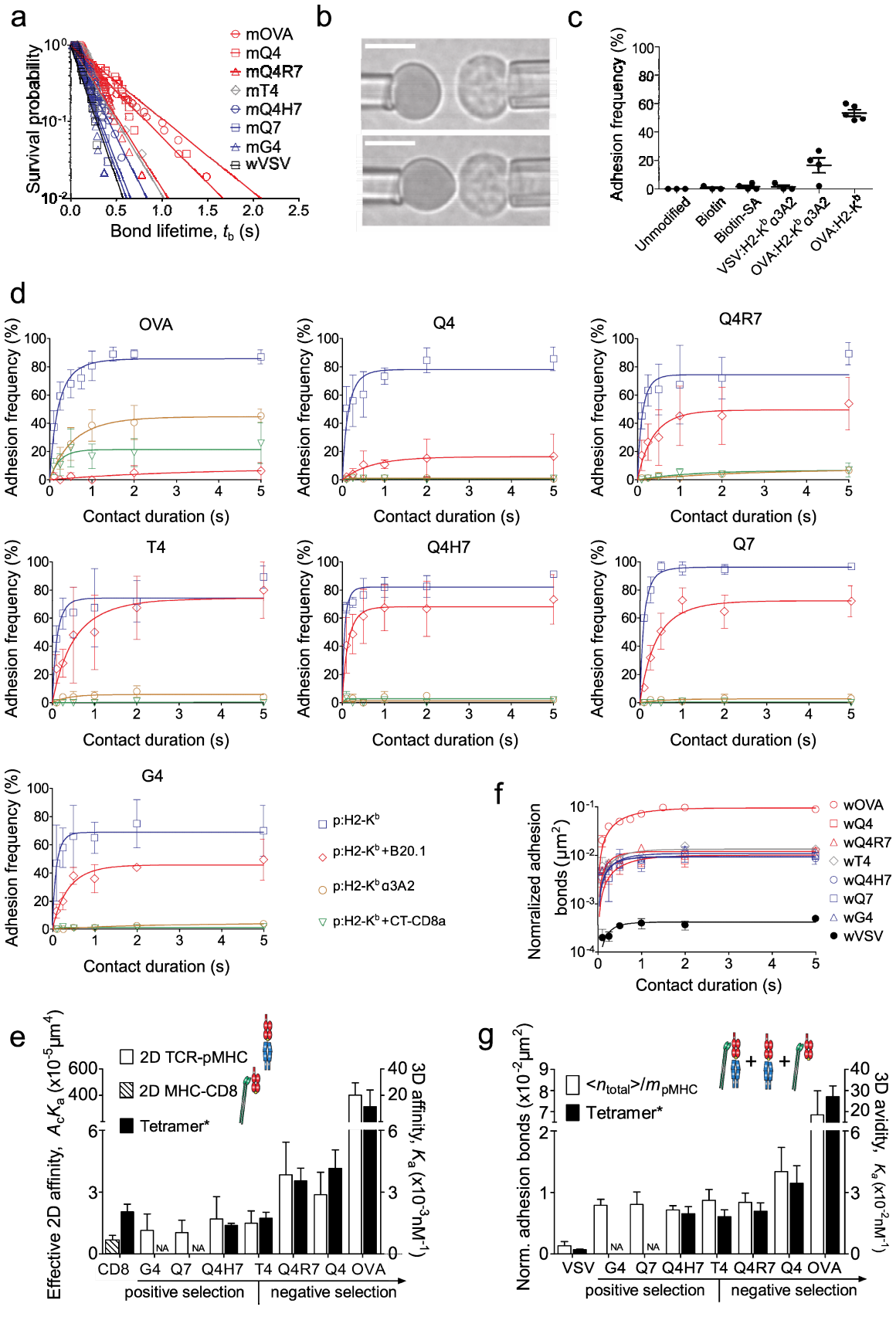
a
Survival probability
Bond lifetime, t_b (s)
mOVA
mQ4
mQ4R7
mT4
mQ4H7
mQ7
mG4
wVSV
b
c
Adhesion frequency (%)
Unmodified
Biotin
Biotin-SA
VSV:H2-K^b α3A2
OVA:H2-K^b α3A2
OVA:H2-K^b
d
OVA
Q4
Q4R7
T4
Q4H7
Q7
G4
Adhesion frequency (%)
Contact duration (s)
p:H2-K^b
p:H2-K^b+B20.1
p:H2-K^b α3A2
p:H2-K^b+CT-CD8a
f
Nomralized adhesion bonds (μm^2)
Contact duration (s)
wOVA
wQ4
wQ4R7
wT4
wQ4H7
wQ7
wG4
wVSV
e
Effective 2D affinity, A_cK_a (x10^{-5}μm^4)
3D affinity, K_a (x10^{-3}nM^{-1})
2D TCR-pMHC
2D MHC-CD8
Tetramer*
NA
CD8 G4 Q7 Q4H7 T4 Q4R7 Q4 OVA
positive selection
negative selection
g
Norm. adhesion bonds (x10^{-2}μm^2)
3D avidity, K_a (x10^{-2}nM^{-1})
<n_{total}>/m_{pMHC}
Tetramer*
VSV G4 Q7 Q4H7 T4 Q4R7 Q4 OVA
positive selection
negative selection

Supplementary Figure 3

2D binding at zero force does not provide clear criteria for thymocyte negative selection, Related to Fig. 5.

a, Lifetimes of OT1 TCR bimolecular bonds with the indicated peptides bound to H2-K^{b}α3A2 or of the MHC**–**CD8 bond (wVSV) were measured by the BFP thermal fluctuation assay[24] at zero-force. Their survival probabilities were plotted as fraction of events with a lifetime ≥ t_b vs. lifetime t_b. The number of bond lifetime measurements are: N = 52 (OVA), 39 (Q4), 49 (Q4R7), 26 (T4), 31 (Q4H7), 39 (Q7), 52 (G4), and 20 (VSV). **b**, Micrographs of the micropipette adhesion frequency assay[25]. A DP thymocyte (*right*) aspirated by a pipette was aligned with a RBC held by another pipette (*left*). The two cells were brought into a controlled contact for a given area (A_c) and duration (t_c) and then retracted to detect binding, which was observed by the absence (top, no adhesion) or presence (bottom, adhesion) of RBC elongation. Scale bar = 5 μm. **c**, Specificity control. At 5 s contact, thymocytes adhered to RBCs coated with wOVA (13 μm^{-2}) at higher frequency than those with mOVA (13 μm^{-2}), showing the contribution of CD8 binding, but did not adhere to unmodified RBCs, biotinylated RBCs, and RBCs coated with biotin–SA (4335 μm^{-2}) or mVSV (604 μm^{-2}). Data are presented as mean ± s.e.m. of cell pairs each contacted 50 times to estimate an adhesion frequency. The number of cell pairs are: N = 3 (unmodified), 3 (biotin), 4 (biotin-SA), 3 (mVSV), 4 (mOVA), and 5 (wOVA). **d**, Adhesion frequency P_a vs. contact duration t_c plots for indicated peptides bound to H2-K^{b}α3A2 (brown circle) or H2-K^b in the absence (blue square) or presence of anti-CD8 CT-CD8a (green triangle) or anti-TCR B20.1 (red diamond). Except for OVA whose measurements required a lower pMHC density (14-46 μm^{-2}), a narrow range of pMHC densities (84-240 μm^{-2}) were used to compare DP thymocyte adhesions in indicated conditions for each ligand. MHC–CD8 interaction (measured by using B20.1 to block TCR binding) mediated lower but clearly measureable adhesion frequencies than the total pMHC interactions with TCR and/or CD8. The much lower adhesions mediated by TCR than CD8 result from the 10 times lower expression of TCR than CD8 on DP thymocytes; but TCR still has higher affinities for pMHC than CD8 (cf. panel **e**). Since TCR–pMHC interactions (measured by using H2-K^{b}α3A2 or CT-CD8a blocking to abolish CD8 binding) were nearly undetectable for these peptides with such low pMHC densities, higher ligand densities (840-3739 μm^{-2}) were used to measure their effective 2D affinities, as shown in panel **e**. Data are presented as mean ± s.e.m. of N≥3 cell pairs for 50 touches each pair. The data are representatives from at least two independent experiments per curve. **e**, No significant differences (p>0.5, one-way ANOVA) were observed among effective 2D affinities A_cK_a of TCR for pMHCs of distinctive selection outcomes (left ordinate, open bar, mean ± s.e.m., N≥5). MHC–CD8 A_cK_a (left ordinate, hatched bar, mean ± s.e.m., N=5) and available 3D tetramer values (right ordinate, black bar)[4] are shown for comparison. **f**, To directly compare different ligands, the adhesion frequency data were converted to average number of bonds by $\langle n \rangle = -\ln(1 - P_a)$, normalized by dividing them by the corresponding pMHC density m_{pMHC}, and plotted vs. contact duration t_c. Except for OVA whose curve (red circle) is 1 log higher, the collapsed $\langle n_{total} \rangle / m_{pMHC}$ curves of the other ligands show no significant difference. The $\langle n_{CD8} \rangle / m_{pMHC}$ curve (black filled circle) is lower. **g**, Normalized total adhesion bonds, $\langle n_{total} \rangle / m_{pMHC} = -\ln(1 - P_a)/m_{pMHC}$ (open bar) for the indicated pMHCs (mean ± s.e.m., N≥3) and available 3D tetramer values (black bar)[4] are shown for comparison. No significant differences were found among the middle 6 ligands (p>0.5, one-way ANOVA). The 2D kinetic parameters measured at zero force by adhesion frequency assay and thermal fluctuation assay are summarized in Supplementary Table 6.

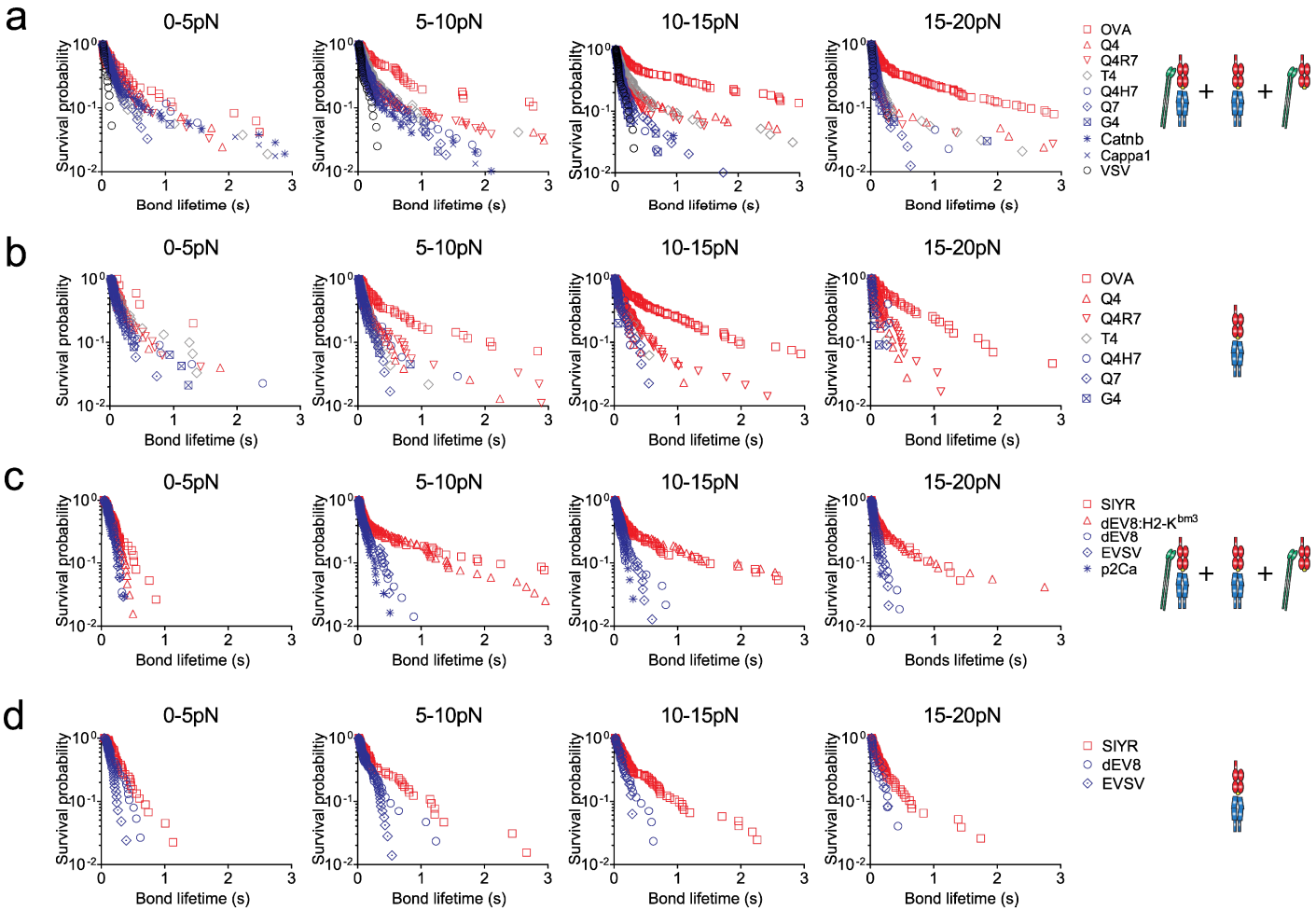

Supplementary Figure 4

Bond lifetime distributions, Related to Fig. 6.

a, **b**, Survival probabilities of total OT1 TCR and/or CD8 bonds with the indicated peptides bound to H2-K^b (**a**) or bimolecular OT1 TCR bonds with the indicated peptides bound to H2-K^{b}α3A2 (**b**) measured by the force-clamp assay in the indicated force regimes. The MHC–CD8 interaction measured using VSV:H2-K^b is shown in black (**a**). **c**, **d**, Survival probabilities of total 2C TCR and/or CD8 bonds with the indicated peptides bound to H2-K^b or H-2K^{bm3} (**c**) or bimolecular 2C TCR bonds with the indicated peptides bound to H2-K^{b}α3A2 (**d**) measured by the thermal fluctuation (0 pN) and force-clamp assay in the indicated force regimes. For the survival probabilities in (a-d), the higher the curve, the slower the dissociation, and the greater the number of bonds surviving a given time. The symbols and legend letters are color-coded to indicate thymocyte selection outcomes: red = negative selection, grey = selection threshold, and blue = positive selection. As force increases, the separation between red and blue curves increased, reached a maximum at 10-15 pN (third column), and then decreased. Separation in lifetime curves was greater for the total bonds that included the synergy between TCR and CD8 for pMHC binding (**a**, **c**) than bimolecular bonds between TCR and pMHC (**b**, **d**).

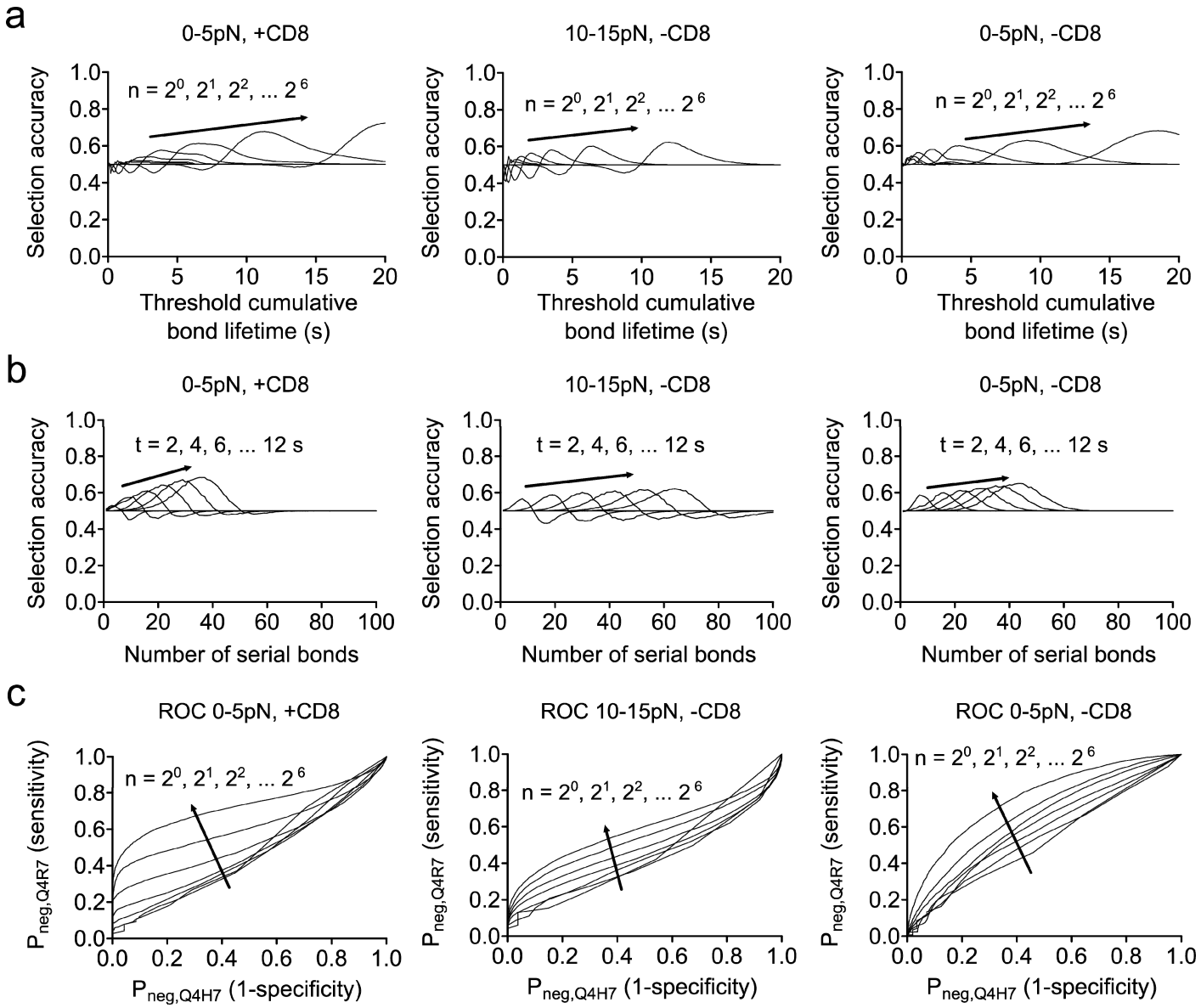

Supplementary Figure 5

Selection accuracy and ROC curves, Related to Fig. 6.

a, Selection accuracy S_A versus threshold cumulative bond lifetime t_{th} for a range of serial bond numbers n. **b**, S_A versus n for a range t_{th} at 0-5 pN with CD8 contribution, at 10-15 pN without CD8 contribution and at 0-5 pN without CD8 contribution. **c**, Receiver operating characteristic (ROC) curves plotting a thymocyte's probability to be negatively selected by wQ4R7 (true-positive rate, or sensitivity) vs. its probability to be negatively selected by wQ4H7 (false-positive rate, or 1 - selectivity) for varying t_{th} and a range of n. The three columns are calculated using the respective bond lifetime distributions of wQ4R7 and wQ4H7 at 0-5 pN, of mQ4R7 and mQ4H7 at 10-15 pN and of mQ4R7 and mQ4H7 at 0-5 pN from Supplementary Fig. 4a, b.

Supplementary Table 1 | Summary of sample sizes of bond lifetime measurements

Number of measurements (N) per bond lifetime vs. force curve are summarized according to the related figures: Fig. 1 (Table 1a), Fig. 4 (Table 1b), Fig. 7 (Table 1c) and Supplementary Fig. 2a (Table 1d).

Supplementary Table 1a, Related to Fig. 1

Figure panel	Interactions and conditions	N
Fig. 1b	Q4H7:H2-K^b vs. OT1	460
Fig. 1b	Q4H7:H2-K^bα3A2 vs. OT1	104
Fig, 1b & Fig. 7b	Q4R7:H2-K^b vs. OT1	694
Fig. 1b	Q4R7:H2-K^bα3A2 vs. OT1	1331
Fig. 1b	VSV:H2-K^b vs. OT1	112
Fig. 1b, c	Q4H7:H2-K^b vs. OT1.CD8.4	648
Fig. 1b, c	Q4H7:H2-K^bα3A2 vs. OT1.CD8.4	379
Fig. 1b, c	Q4R7:H2-K^b vs. OT1.CD8.4	370
Fig. 1b, c	Q4R7:H2-K^bα3A2 vs. OT1.CD8.4	468
Fig. 1b	VSV:H2-K^b vs. OT1.CD8.4	746
Fig. 1c	Q4H7:H2-K^b vs. OT1 + Lck inhibitor	408
Fig. 1c	Q4H7:H2-K^bα3A2 vs. OT1 + Lck inhibitor	399
Fig. 1c	Q4H7:H2-K^b vs. OT1 + DMSO treatment	498
Fig. 1c	Q4R7:H2-K^b vs. OT1 + Lck inhibitor	1351
Fig. 1c	Q4R7:H2-K^bα3A2 vs. OT1 + Lck inhibitor	377
Fig. 1c	Q4R7:H2-K^b vs. OT1 + DMSO treatment	468
Fig. 1c	VSV:H2-K^b vs. OT1 + Lck inhibitor	287
Fig. 1c	Q4H7:H2-K^b vs. OT1.CD8.4 + Lck inhibitor	816
Fig. 1c	Q4H7:H2-K^b vs. OT1.CD8.4 + DMSO treatment	612
Fig. 1c	Q4R7:H2-K^b vs. OT1.CD8.4 + Lck inhibitor	356

Supplementary Table 1b, Related to Fig. 4

Figure panel	Interactions and conditions	N
Fig. 4a	OVA:H2-K^b vs. OT1	707
Fig. 4a	OVA:H2-K^bα3A2 vs. OT1	375
Fig. 4a & Fig. 7b	Q4:H2-K^b vs. OT1	506
Fig. 4a	Q4:H2-K^bα3A2 vs. OT1	214
Fig. 4a	T4:H2-K^b vs. OT1	620
Fig. 4a	T4:H2-K^bα3A2 vs. OT1	109
Fig. 4a	Q7:H2-K^b vs. OT1	401
Fig. 4a	Q7:H2-K^bα3A2 vs. OT1	154
Fig. 4a	G4:H2-K^b vs. OT1	157
Fig. 4a	G4:H2-K^bα3A2 vs. OT1	118
Fig. 4b	Catnb329-336:H2-K^b vs. OT1	230
Fig. 4b	Cappa192-99:H2-K^b vs. OT1	242
Fig. 4a, b	VSV:H2-K^b vs. OT1	112

Supplementary Table 1c, Related to Fig. 7

Figure panel	Interactions and conditions	N
Fig. 7a, b	Q4R7:H2-K^b vs. OT1.6F	922
Fig. 7a	Q4R7:H2-K^bα3A2 vs. OT1.6F	694
Fig. 7a, b	Q4:H2-K^b vs. OT1.6F	538
Fig. 7a	Q4:H2-K^bα3A2 vs. OT1.6F	867
Fig. 7a, b	VSV:H2-K^b vs. OT1.6F	399

Supplementary Table 1d, Related to Supplementary Fig. 2a

Figure panel	Interactions and conditions	N
Supplementary Fig. 2a	SIYR:H2-K^b vs. 2C	360
Supplementary Fig. 2a	SIYR:H2-K^bα3A2 vs. 2C	363
Supplementary Fig. 2a	dEV8:H2-K^b vs. 2C	184
Supplementary Fig. 2a	dEV8:H2-K^bα3A2 vs. 2C	187
Supplementary Fig. 2a	EVSV:H2-K^b vs. 2C	187
Supplementary Fig. 2a	EVSV:H2-K^b α3A2vs. 2C	187
Supplementary Fig. 2a	dEV8:H2-K^bm3 vs. 2C	402
Supplementary Fig. 2a	p2Ca:H2-K^b vs. 2C	151
Supplementary Fig. 2a	VSV:H2-Kb vs. 2C	112

Supplementary Table 2 | Statistical tests of dynamic bond types

Statistical tests of dynamic bond types are summarized according to the related figures: Fig. 1 (Table 2a), Fig. 4 (Table 2b), Supplementary Fig. 2a (Table 2c) and Fig. 7 (Table 2d). Each biphasic bond lifetime vs. force curve was divided into two segments with monotonic trends and the ascending segment was linearly regressed to obtain a slope. Each monophasic bond lifetime vs. force curve with a monotonic descending trend was also linearly regressed to obtain a slope. Two-sided Student's t-test was used to assess the significance of these slopes. Null hypothesis = Slope is not greater (for catch bond) or not smaller (for slip bond) than zero. Alternative hypothesis = Slope is greater (for catch bond) or smaller (for slip bond) than zero. When there was only two force bins in an ascending trend, unpaired Student's t-test was used to assess the significance of the trend.

Supplementary Table 2a, Related to Fig. 1

Figure panel	Interactions and conditions	Trend	p-value
Fig. 1b	wQ4H7 vs. OT1	Slip	0.0001, ****
Fig. 1b	mQ4H7 vs. OT1	Slip	0.0065, **
Figs. 1b, 4a, S2a	wVSV vs. OT1	Slip	0.0614, NS
Fig. 1b	wQ4R7 vs. OT1	Catch	0.0072, **
Fig. 1b	mQ4R7 vs. OT1	Slip	0.0013, **
Fig. 1b, c	wQ4H7 vs. OT1.CD8.4	Catch	0.0401, *
Fig. 1b, c	mQ4H7 vs. OT1.CD8.4	Slip	0.0511, NS
Fig. 1b, c	wQ4R7 vs. OT1.CD8.4	Catch	0.0123, *
Fig. 1b, c	mQ4R7 vs. OT1.CD8.4	Slip	0.0098, **
Fig. 1c	wQ4H7 vs. OT1 + DMSO treatment	Slip	0.0045, **
Fig. 1c	wQ4H7 vs. OT1 + Lck inhibitor	Slip	0.0016, **
Fig. 1c	mQ4H7 vs. OT1 + Lck inhibitor	Slip	0.0033, **
Fig. 1c	wVSV vs. OT1 + Lck inhibitor	Slip	0.0604, NS
Fig. 1c	wQ4R7 vs. OT1 + DMSO treatment	Catch	0.0001, ****
Fig. 1c	wQ4R7 vs. OT1 + Lck inhibitor	Slip	0.0006, ***
Fig. 1c	mQ4R7 vs. OT1 + Lck inhibitor	Slip	0.0280, *
Fig. 1c	wQ4H7 vs. OT1.CD8.4 + DMSO treatment	Catch	0.0076, **
Fig. 1c	wQ4H7 vs. OT1.CD8.4 + Lck inhibitor	Slip	0.0008, ***
Fig. 1c	wQ4R7 vs. OT1.CD8.4 + Lck inhibitor	Catch	0.0151, *

NS = Not Significance (i.e., the slopes of the descending trend in the above three cases are not significantly smaller than zero, so these could be ideal bonds instead of slip bonds).

Supplementary Table 2b, Related to Fig. 4

Figure panel	Interactions and conditions	Trend	p-value
Fig. 4a	wOVA vs. OT1	Catch	0.0098, **
Fig. 4a	mOVA vs. OT1	Catch	0.0312, *
Fig. 4a	wQ4 vs. OT1	Catch	0.0228, *
Fig. 4a	mQ4 vs. OT1	Slip	0.0129, *
Fig. 4a	wT4 vs. OT1	Catch	0.0415, *
Fig. 4a	mT4 vs. OT1	Slip	0.0112, *
Fig. 4a	wQ7 vs. OT1	Slip	0.0005, ***
Fig. 4a	mQ7 vs. OT1	Slip	0.0864, NS
Fig. 4a	wG4 vs. OT1	Slip	0.0002, ***
Fig. 4a	mG4 vs. OT1	Slip	0.0043, **
Fig. 4b	Catnb329-336 vs. OT1	Slip	0.0904, NS
Fig. 4b	Cappa192-99 vs. OT1	Slip	0.0747, NS

NS = Not Significance (i.e., the slopes of the descending trend in the above three cases are not significantly smaller than zero, so these could be ideal bonds instead of slip bonds).

Supplementary Table 2c, Related to Supplementary Fig. 2

Figure panel	Interactions and conditions	Trend	p-value
Fig. S2a	wSIYR vs. 2C	Catch[‡]	0.0435, *
Fig. S2a	mSIYR vs. 2C	Catch	0.0615, NS
Fig. S2a	wdEV8 vs. 2C	Slip	0.0304, *
Fig. S2a	mdEV8 vs. 2C	Slip	0.0021, **
Fig. S2a	wEVSV vs. 2C	Slip	0.0053, **
Fig. S2a	mEVSV vs. 2C	Slip	0.0026, **
Fig. S2a	dEV8:H2-K^{bm3} vs. 2C	Catch	0.0261, *
Fig. S2a	P2Ca:H2-K^{b} vs. 2C	Slip	0.0031, **

NS = Not Significance (i.e., the slope of the ascending trend in the above case is not significantly greater than zero, so the apparent catch-slip bond could be an ideal-slip bond).
[‡]The first two force points of the bond lifetime vs. force curve showed a descending trend but not significant. Points 2-4 exhibited a significant ascending trend. Thus, this is a catch-slip bond case.

Supplementary Table 2d, Related to Fig. 7

Figure panel	Interactions and conditions	Trend	p-value
Fig. 7a, b	wQ4R7 vs. OT1.6F	Catch	0.0122, *
Fig. 7a	mQ4R7 vs. OT1.6F	Slip	0.0002, ***
Fig. 7a, b	wVSV vs. OT1.6F	Slip	0.0290, *
Fig. 7a, b	wQ4 vs. OT1.6F	Catch	0.0263, *
Fig. 7a	mQ4 vs. OT1.6F	Slip	0.0008, ***
Fig. 7b (1b)	wQ4R7 vs. OT1	Catch	0.0072, **
Fig. 7b (4a)	wQ4 vs. OT1	Catch	0.0228, *

Supplementary Table 3 | Statistical comparisons of two bond lifetime vs. force curves

Statistical comparisons of two bond lifetime vs. force curves are summarized according to the types of comparison: comparison between two slip-only bond curves (Table 3a), comparison between two curves with at least one curve showing catch-slip bond (Table 3b) and comparison between two catch-slip bonds (Table 3c).

Supplementary Table 3a. Comparison between two slip-only bond curves, Related to Fig. 1, 4, and Supplementary Fig. 2

Figure panel	Thymocyte	Interactions and conditions	p-value
Fig. 1b	OT1	wQ4H7 (slip) vs. mQ4H7 (slip)	0.4718, NS
Fig. 1c	OT1	wQ4H7, Lck inhibitor (slip) vs. DMSO (slip)	<0.0001
Fig. 4a	OT1	wQ7 (slip) vs. mQ7 (slip)	0.7168, NS
Fig. 4a	OT1	wG4 (slip) vs. mG4 (slip)	0.7745, NS
Fig. S2a	2C	wdEV8 (slip) vs. mdEV8 (slip)	0.7258, NS
Fig. S2a	2C	wEVSV (slip) vs. mEVSV (slip)	0.4119, NS

Null hypothesis = The two data sets are not different.
Alternative hypothesis = The two data sets are different.
Unpaired two-way ANOVA was used to assess the significance of the difference.

Supplementary Table 3b. Comparison between two curves with at least one curve showing catch-slip bond, Related to Fig. 1, 4, 7 and Supplementary Fig. 2

Figure panel	Thymocyte	Interactions and conditions	p-value
Fig. 1b	OT1	wQ4R7 (catch) vs. mQ4R7 (slip)	0.000000061, ***
Fig. 1b	OT1.CD8.4	wQ4H7 (catch) vs. mQ4H7 (slip)	0.000062, ***
Fig. 1b	OT1.CD8.4	wQ4R7 (catch) vs. mQ4R7 (slip)	0.000046, ***
Fig. 1c	OT1	wQ4R7, DMSO (catch) vs. Lck inhibitor (slip)	0.0000000039, ***
Fig. 1c	OT1.CD8.4	wQ4H7, Lck inhibitor (slip) vs. DMSO (catch)	<2e-16, *********
Fig. 1c	OT1.CD8.4	wQ4R7, untreated (catch) vs. Lck inhibitor (catch)	0.87
Fig. 4a	OT1	wOVA (catch) vs. mOVA (catch)	0.026, *
Fig. 4a	OT1	wQ4 (catch) vs. mQ4 (slip)	0.0013, **
Fig. 4a	OT1	wT4 (catch) vs. mT4 (slip)	0.0006, ***
Fig. 7a	OT1.6F	wQ4R7 (catch) vs. mQ4R7 (slip)	0.00045, ***
Fig. 7a	OT1.6F	wQ4 (catch) vs. mQ4 (slip)	0.0013, **
Fig. S2a	2C	wSIYR (catch) vs. mSIYR (catch)	0.41
Fig. S2a	2C	dEV8:H2-K^{bm3} (catch) vs. dEV8:H2-Kb (slip)	0.035, *

Null hypothesis = The two data sets are not different.
Alternative hypothesis = The two data sets are different.
An accelerated failure time model was used to compare the mean lifetimes between the two curves over a range of forces. The scatter bond lifetime data points were binned according to their force levels and lifetime distributions in each force bin were fitted by Weibull distributions. A penalized spline smoothing function was used to fit the nonlinear mean bond lifetime vs. force curve. The

difference in nonlinear patterns between groups was compared based on the significance of group and force level interaction terms (including spline terms).

Supplementary Table 3c, Comparison between two catch-slip bonds, Related to Fig. 7

Panel	Condition	Optimal force shift p-value	Slip phase shift p-value
Fig. 7b	wQ4R7 on OT1.6F vs on OT1	1.66938e-83, **********	0.026264, *
Fig. 7b	wQ4 on OT1.6F vs on OT1	2.78398e-22, **********	0.017219, *

The mean forces where mean bond lifetime peaked in the two curves were compared using two-sample t-test to examine whether the two peak locations (of force) are different. The slip phases of two bond lifetime vs. binned force curves were compared for their relative shift. Each curve was fitted with quadratic regression, weighted by the reciprocal of standard-error of each bin. Significance level of the shift was evaluated by two-sided Student's t-test.

Supplementary Table 4 | Summary of fitting parameters of molecular stiffness histograms

Fitting parameters of molecular stiffness histograms are summarized according to single- (for OT1, Table 4a and for 2C, Table 4c) or double-Gaussian (for OT1, Table 4b and for 2C, Table 4d) fitting.

Supplementary Table 4a. OT1 Single-Gaussian fit, Related to Figs. 2, 4, and Supplementary Fig. 1

Panel	Interaction and conditions	Mean	SD	Amplitude	N
Fig. 2g	mQ4H7 vs. OT1	0.063	0.177	0.267	25
Fig. 2g	wQ4H7 vs. OT1	0.185	0.195	0.215	82
Fig. 2g	mQ4R7 vs. OT1	0.230	0.290	0.156	103
Fig. 2g	mQ4H7 vs. OT1.CD8.4	0.203	0.227	0.195	61
Fig. 2g	mQ4R7 vs. OT1.CD8.4	0.212	0.163	0.260	77
Fig. 2g	mQ4H7 vs. OT1 + Lck inhibition	0.163	0.126	0.332	28
Fig. 2g	wQ4H7 vs. OT1 + Lck inhibition	0.147	0.103	0.382	41
Fig. 2g	mQ4R7 vs. OT1 + Lck inhibition	0.218	0.134	0.311	34
Fig. 2g	wQ4R7 vs. OT1 + Lck inhibition	0.204	0.135	0.306	74
Supplementary Fig. 1	wQ4H7 vs. OT1 + DMSO treatment	0.242	0.101	0.399	37
Supplementary Fig. 1	wQ4H7 vs. OT1.CD8.4 + Lck inhibition	0.218	0.125	0.315	37
Fig. 4c	mOVA vs. OT1	0.295	0.276	0.141	93
Fig. 4c	mQ4 vs. OT1	0.176	0.192	0.209	76
Fig. 4c	mT4 vs. OT1	0.112	0.130	0.244	52
Fig. 4c	mQ7 vs. OT1	0.075	0.275	0.220	34
Fig. 4c	mG4 vs. OT1	0.177	0.165	0.265	23
Fig. 4d	wQ7 vs. OT1	0.123	0.209	0.221	62
Fig. 4d	wG4 vs. OT1	0.178	0.137	0.292	63

Supplementary Table 4b. OT1 Double-Gaussian fit, Related to Figs. 2, 4, and Supplementary Fig. 1

Figure Panel	Interaction and conditions	1st mean	1st SD	1st Amplitude	2nd mean	2nd SD	2nd Amplitude	N
Fig. 2g	wQ4R7 vs. OT1	0.189	0.140	0.083	0.389	0.597	0.061	254
Fig. 2g	wQ4H7 vs. OT1.CD8.4	0.140	0.065	0.160	0.258	0.583	0.066	221
Fig. 2g	wQ4R7 vs OT1.CD8.4	0.175	0.184	0.131	1.092	0.425	0.038	177
Supplementary Fig. 1	wQ4R7 vs. OT1 + DMSO treatment	0.194	0.117	0.150	0.551	0.361	0.063	106
Supplementary Fig. 1	wQ4R7 vs. OT1.CD8.4 + Lck inhibition	0.183	0.051	0.150	0.414	0.274	0.121	46
Supplementary Fig. 1	wQ4H7 vs. OT1.CD8.4 + DMSO treatment	0.182	0.165	0.178	0.739	0.061	0.118	56
Fig. 4d	wOVA vs. OT1	0.192	0.165	0.073	0.564	0.451	0.064	192
Fig. 4d	wQ4 vs. OT1	0.202	0.327	0.093	0.921	0.706	0.021	162
Fig. 4d	wT4 vs. OT1	0.136	0.175	0.078	0.316	0.594	0.063	197

Supplementary Table 4c. 2C Single-Gaussian fit, Related to Supplementary Fig. 2b

Panel	Interaction and conditions	Mean	SD	Amplitude	N
Supplementary Fig. 2b	mSIYR vs. 2C	0.216	0.170	0.247	138
Supplementary Fig. 2b	mdEV8 vs. 2C	0.230	0.142	0.297	26
Supplementary Fig. 2b	mEVSV vs. 2C	0.220	0.132	0.315	37
Supplementary Fig. 2b	wdEV8 vs. 2C	0.250	0.170	0.254	51
Supplementary Fig. 2b	wEVSV vs. 2C	0.182	0.088	0.453	25
Supplementary Fig. 2b	wp2Ca vs. 2C	0.176	0.173	0.244	78

Supplementary Table 4d. 2C Double-Gaussian fit, Related to Supplementary Fig. 2b

Figure Panel	Interaction and conditions	1st mean	1st SD	1st Amplitude	2nd mean	2nd SD	2nd Amplitude	N
Supplementary Fig. 2b	wSIYR vs. 2C	0.208	0.133	0.183	0.590	0.326	0.048	158
Supplementary Fig. 2b	wdEV8:bm3 vs. 2C	0.173	0.108	0.167	0.500	0.255	0.076	114

Supplementary Table 5 | Statistical comparisons of molecular stiffness histogram fits

To determine whether the single or double Gaussian model better fits the molecular stiffness histograms of total bonds. The goodness-of-fit of these models were assessed by the extra sum-of-squares F-test. Null hypothesis: Single Gaussian fits the distribution better. Alternative hypothesis: Double Gaussian fits the distribution better.

Supplementary Table 5a, Related to Fig. 2 and Supplementary Fig. 1

Figure panel	Interaction and conditions	p-values from the extra sum-of-squares F-test
Fig. 2f	wVSV vs. OT1	0.1364
Fig. 2f	wVSV vs. OT1.CD8.4	0.3492
Fig. 2g	mQ4H7 vs. OT1	0.0853
Fig. 2g	wQ4H7 vs. OT1	0.2783
Fig. 2g	mQ4R7 vs. OT1	0.0901
Fig. 2g	wQ4R7 vs. OT1	0.0012 (**)
Fig. 2g	mQ4H7 vs. OT1.CD8.4	0.0963
Fig. 2g	wQ4H7 vs. OT1.CD8.4	< 0.0001 (****)
Fig. 2g	mQ4R7 vs. OT1.CD8.4	0.1435
Fig. 2g	wQ4R7 vs. OT1.CD8.4	0.0104 (*)
Fig. 2g	mQ4H7 vs. OT1 + Lck inhibition	0.9997
Fig. 2g	wQ4H7 vs. OT1 + Lck inhibition	0.9349
Fig. 2g	mQ4R7 vs. OT1 + Lck inhibition	0.9605
Fig. 2g	wQ4R7 vs. OT1 + Lck inhibition	0.3309
Supplementary Fig. 1	wQ4H7 vs. OT1 + DMSO treatment	0.4634
Supplementary Fig. 1	wQ4R7 vs. OT1 + DMSO treatment	0.0003 (***)
Supplementary Fig. 1	wQ4H7 vs. OT1.CD8.4 + Lck inhibition	0.0747
Supplementary Fig. 1	wQ4R7 vs. OT1.CD8.4 + Lck inhibition	< 0.0001 (****)
Supplementary Fig. 1	wQ4H7 vs. OT1.CD8.4 + DMSO treatment	0.0057 (**)

Supplementary Table 5b, Related to Fig. 4

Figure panel	Interaction and conditions	p-values from the extra sum-of-squares F-test
Fig. 4c	mOVA vs. OT1	0.0502
Fig. 4c	mQ4 vs. OT1	0.1315
Fig. 4c	mT4 vs. OT1	0.1458
Fig. 4c	mQ7 vs. OT1	0.0753
Fig. 4c	mG4 vs. OT1	0.4820
Fig. 4d	wOVA vs. OT1	0.0259 (*)
Fig. 4d	wQ4 vs. OT1	0.0126 (*)
Fig. 4d	wT4 vs. OT1	0.0025 (**)
Fig. 4d	wQ7 vs. OT1	0.0829
Fig. 4d	wG4 vs. OT1	0.1639

Supplementary Table 5c, Related to Supplementary Fig. 2b

Figure panel	Interaction and conditions	p-values from the extra sum-of-squares F-test
Supplementary Fig. 2b	mSIYR vs. 2C	0.0820
Supplementary Fig. 2b	mdEV8 vs. 2C	0.2168
Supplementary Fig. 2b	mEVSV vs. 2C	0.1003
Supplementary Fig. 2b	wSIYR vs. 2C	< 0.0001 (****)
Supplementary Fig. 2b	wdEV8 vs. 2C	0.1840
Supplementary Fig. 2b	wEVSV vs. 2C	0.5138
Supplementary Fig. 2b	wdEV8:bm3 vs. 2C	0.0028 (**)
Supplementary Fig. 2b	wp2Ca vs. 2C	0.9076

Supplementary Table 6. Summary of zero-force kinetic parameters, Related to Supplementary Fig. 3

Effective 2D on-rate, 2D off-rate, effective 2D affinity and normalized adhesion bonds were measured using adhesion frequency assay.

	Effective 2D on-rate, $A_c k_{on}$ ($\mu m^4 s^{-1}$)	**SEM**	**N**	**2D off-rate, k_{off} (s^{-1})**	**SEM**	**N**
CD8	0.000040	2.38E-05	5	6.982	0.815	20
G4	0.000054	3.82E-05	4	4.737	0.501	52
Q7	0.000046	2.74E-05	4	4.427	0.456	39
Q4H7	0.000071	4.60E-05	5	4.164	0.475	31
T4	0.000059	2.51E-05	17	3.983	0.463	26
Q4R7	0.000135	5.68E-05	10	3.526	0.291	49
Q4	0.000090	3.51E-05	7	3.129	0.288	39
OVA	0.011303	3.06E-03	5	2.830	0.377	52

	Effective 2D Affinity, $A_c K_a$ (μm^4)	**SEM**	**N**	**Normalized adhesion bonds (μm^2)**	**SEM**	**N**
CD8	5.73E-06	3.34E-06	5	0.00134	0.00070	3
G4	1.14E-05	7.98E-06	4	0.00793	0.00097	2
Q7	1.03E-05	6.09E-06	4	0.00805	0.00203	5
Q4H7	1.70E-05	1.09E-05	5	0.00716	0.00069	4
T4	1.49E-05	6.07E-06	17	0.00872	0.00178	5
Q4R7	3.84E-05	1.58E-05	10	0.00840	0.00150	5
Q4	2.87E-05	1.09E-05	7	0.01337	0.00394	7
OVA	3.99E-03	9.41E-04	5	0.06840	0.01149	6